

Large-angle scattering of energetic electrons from Xe: A combined theoretical and experimental approach

R. P. McEachran and M. Vos

*Atomic and Molecular Physics Laboratories, Research School of Physics and Engineering, Australian National University,
Canberra ACT, Australia*

(Received 30 November 2011; published 2 March 2012)

We study the inelastic excitations of Xe for electrons with relatively high energies (500 or 750 eV) scattered over large angles, both experimentally and theoretically. In particular, we focus on the shape and intensity of the spectra of *inelastically* scattered electrons at the sharp dip in the *elastic* cross section near 135° at 750 eV. Under these conditions, the first Born approximation predicts virtually zero intensity. However, in reality, measurable intensity is observed. Calculations carried out using the relativistic distorted-wave method describe the measurements reasonably well. A comparison is made between the calculations and previously published high-resolution studies. Overall agreement is quite good, especially for the lowest-energy excitations, but substantial differences are found for certain higher levels. The theory reproduces quite well the variations in intensity of the inelastic excitations for measurements near the dip in the elastic-scattering cross section, somewhat surprisingly, as the theories for elastic scattering and inelastic scattering are developed along completely different lines.

DOI: [10.1103/PhysRevA.85.032703](https://doi.org/10.1103/PhysRevA.85.032703)

PACS number(s): 34.80.Dp

I. INTRODUCTION

Understanding the propagation of keV electrons in materials is pivotal for the interpretation of electron spectroscopy data of surfaces. The trajectories are usually described by deflections from nuclei (elastic scattering) and electronic excitations (inelastic scattering). These two processes are considered to be independent. Elastic scattering is considered to be well approximated by scattering from (isolated) atoms that comprise the solid, while inelastic scattering depends strongly on the electronic structure of the valence band of the solid.

Elastic and inelastic scattering of electrons from molecules and atoms are, thus, usually considered two separate topics. Our knowledge of elastic-scattering cross sections is largely based on theoretical calculations, which have been tested for those elements that can be studied easily in the gas phase, i.e., noble gases and high-vapor pressure metals such as Cd and Hg; see e.g., Ref. [1]. In our previous work [2], we studied electron scattering from Xe. This element has a sharp minimum in the differential cross section at 750 eV near 135° . It was, thus, somewhat of a surprise that the shape of the spectra of inelastic scattered electrons show huge variations when the energy of the incoming beam is tuned to the sharp minimum of the elastic cross section for that scattering angle [2]. Clearly, under these conditions, the intensity of the inelastically scattered electrons is not due to interactions between the projectile and target electrons only, but that the target nucleus is involved as well. Indeed, any theory based on the first Born approximation predicts only negligible intensity under these scattering conditions. Moreover, near the minimum of the elastic cross section, the intensity of the energy loss part of the spectrum was not small compared to the intensity of the elastic peak. This makes the usual interpretation of electron spectroscopy data questionable, especially when scattering angles near a minimum in the elastic cross section are considered, as in certain reflection electron energy loss (REELS) experiments [3].

In this paper we revisit this problem and study the inelastic-scattering cross section dependence on the scattering angle θ and use a relativistic distorted-wave (RDW) approach to calculate the spectra under these conditions. This theory was used before to describe the spectra of electrons scattered inelastically with energies between 0.3 and 2.5 keV from Ar and Ne [4]. For small scattering angles, this theory coincides with the first Born approximation (FBA), but at larger scattering angles its intensity exceeds that of the FBA by many orders of magnitude. Good agreement was obtained between theory and experiment for the intensity of the lowest excitation levels of Ar and Ne. We now extend these calculations to the case of Xe with the aim of obtaining a better understanding of the peculiar behavior of the inelastic spectra near a minimum in the elastic cross section.

II. EXPERIMENT

The experimental technique used was described extensively in Ref. [2] and is only summarized here. Electrons emitted from a BaO cathode and with an energy of the order of 1 keV are scattered from Xe atoms effusing out of a needle. The scattered electrons are decelerated and energy analyzed by an electrostatic analyzer. The combined energy resolution (gun plus analyzer) is 0.3 eV. The gun can be mounted on flanges at 45° , 90° , or 135° relative to the analyzer. It was checked visually that the error in the alignment of these ports was less than 0.5° .

In Ref. [2] we observed the effect of a sharp resonance in the cross section near $\theta = 135^\circ$ for 750 eV electrons by varying the incoming energy E_0 . In order to study this minimum as a function of θ , we added a set of deflectors to our spectrometer, right before the last aperture, as shown in Fig. 1. This deflector is used to change the direction of the beam in the interaction region and, hence, change the scattering angle by up to $\pm 5^\circ$. In this way, we can change the scattering angle to any value between 130° and 140° , thereby probing the region of the

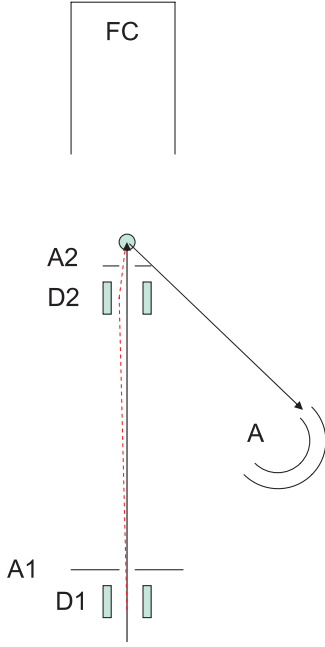


FIG. 1. (Color online) Schematic working of the deflectors. Without the deflectors the electron trajectory follows the solid line, with deflector voltages applied it follows the dotted line. A1 and A2 denote apertures 1 and 2; D1 and D2 denote deflectors 1 and 2; F.C. denotes Faraday cup; A denotes analyzer.

sharp minimum in the elastic-scattering cross section near 135° at 750 eV. The dependence of the deflection angle on the deflector voltage was determined using the SIMION electron optics package [5].

III. THEORY

In this work, the inelastic differential cross sections were calculated using the relativistic distorted-wave (RDW) method while the elastic cross sections were determined using a relativistic optical potential (ROP) method. Both of these methods have recently been described (see Ref. [4], hereafter referred to as I) in connection with similar types of calculations in neon and argon. Consequently, only a brief description of these procedures, with particular regard to xenon, will be given here.

A. The RDW method

The Dirac-Fock wave functions of the target atom were determined using the multiconfiguration Dirac-Fock programme of Grant *et al.* [6]. The ground-state wave function for xenon was determined from a single configuration while, in general, the excited-state wave functions, with the same total angular-momentum value J , were determined in a multiconfiguration approach. In the scattering experiment, the incoming electron (momentum \mathbf{k}_a) scatters over an angle θ and is detected with momentum \mathbf{k}_b . If we now denote (in intermediate coupling notation) the excited states of a noble gas by $n'\kappa'[K]_J^P$, then

the total differential cross section $\sigma_{n'\kappa'}^{JK}(\hat{\mathbf{k}}_b)$ for the excitation of this state from the ground state is given by

$$\sigma_{n'\kappa'}^{JK}(\hat{\mathbf{k}}_b) = \frac{1}{2} \sum_{M=-J}^J \sum_{\mu_a \mu_b} |f_{n'\kappa'}^{JK}(M, \mu_a, \mu_b; \hat{\mathbf{k}}_b)|^2, \quad (1)$$

where $f_{n'\kappa'}^{JK}(M, \mu_a, \mu_b; \hat{\mathbf{k}}_b)$ is the scattering amplitude which, in turn, can be expressed in terms of the corresponding T -matrix element by

$$f_{n'\kappa'}^{JK}(M, \mu_a, \mu_b; \hat{\mathbf{k}}_b) = (2\pi)^2 \left(\frac{k_b}{k_a}\right)^{\frac{1}{2}} T_{n'\kappa'}^{JK}(M, \mu_a, \mu_b; \hat{\mathbf{k}}_b). \quad (2)$$

In the above equations, J and M are the total angular-momentum quantum numbers of the excited state; P is the parity of the state; μ_a, μ_b are the magnetic spin projection quantum numbers of the incident and outgoing electrons; and $\hat{\mathbf{k}}_b$ specifies the direction of the outgoing electron. The quantum number κ is defined in terms of the orbital and total angular-momentum quantum numbers (l, j) of an electron by $\kappa = -l - 1$ for $j = l + \frac{1}{2}$ and $\kappa = l$ for $j = l - \frac{1}{2}$. Finally, the T -matrix elements in Eq. (2) are expressed in terms of relativistic distorted waves according to Eq. (3) of I. These distorted waves are, in turn, determined from the solution of the Dirac scattering equation given by Eqs. (9a) and (9b) of I. In the solution of these equations, the distortion potential U was chosen to be the ground-state static potential in the initial channel and the excited-state static potential in the final channel.

The spectra, we present later, were calculated from a total of 79 excited states of the form $n'\kappa'[K]_J^P$, where the principal and angular-momentum quantum numbers $n'\kappa'$ were given by $n's$, $n'\bar{p}$ ($j = \frac{1}{2}$), $n'p$ ($j = \frac{3}{2}$), $n'\bar{d}$ ($j = \frac{3}{2}$), and $n'd$ ($j = \frac{5}{2}$) electrons. For s electrons, states with $n' = 6$ to 12, $J = 1$, and odd parity were included. Similarly, for \bar{p} and p electrons, states with $n' = 6$ to 12, $J = 0, 2$, and even parity were included while for \bar{d} and d electrons, states with $n' = 5$ to 12, $J = 1, 3$, and odd parity were included. All of the above states include both direct and exchange T -matrix elements [see Eq. (3) of I]. The intensity of those excited states whose J value was such that only the exchange T -matrix element was nonzero are several orders of magnitude smaller at these high energies.

B. The ROP method

The elastic differential cross section for the ground state of xenon was calculated using the ROP method of Chen *et al.* [10]. Here the optical potential is both complex and *ab initio*, the real part of which, U_{pol} , describes the polarization of the target atom by the incident electron while the imaginary part, U_{abs} , describes the loss of incident flux into excitation and ionization channels. As in I, we use our local polarized-orbital polarization potential, containing both static and dynamic terms, for U_{pol} . The precise form of these potentials are discussed in McEachran and Stauffer (Refs. [11,12] and references therein). The nonlocal imaginary absorption potential was determined from an expansion over the inelastic channels of the target atom. These inelastic channels included both the

excitation of bound states as well as the single ionization of the target atom. In particular, 15 excitation channels and 35 ionization channels of xenon, again involving s , \bar{p} , p , \bar{d} , and d electrons, were included.

The complex phase shifts δ_l^\pm were determined from the solution of the Dirac scattering equations [Eq. (11)] of I. From these phase shifts, the direct and spin-flip scattering amplitudes, $f(\theta)$ and $g(\theta)$, respectively, can be calculated in terms of the T -matrix elements according to

$$f(\theta) = \frac{1}{k_0} \sum_{l=0}^{\infty} [(l+1) T_l^+(k_0) + l T_l^-(k_0)] P_l(\cos \theta) \quad (3)$$

and

$$g(\theta) = \frac{1}{k_0} \sum_{l=0}^{\infty} [T_l^-(k_0) - T_l^+(k_0)] P_l^1(\cos \theta), \quad (4)$$

where $P_l(\cos \theta)$ and $P_l^1(\cos \theta)$ are the Legendre and associated Legendre polynomials and

$$T_l^\pm(k_0) = \frac{1}{2i} \{\exp[2i \delta_l^\pm(k_0)] - 1\}. \quad (5)$$

Here T_l^+ is the T -matrix element corresponding to spin-up ($\kappa < 0$, $j = l + \frac{1}{2}$) while T_l^- corresponds to spin-down ($\kappa > 0$, $j = l - \frac{1}{2}$) and k_0 is the wave number of the incident electron. In terms of these scattering amplitudes, the elastic differential cross section $\sigma(\theta)$ is given by

$$\sigma(\theta) = |f(\theta)|^2 + |g(\theta)|^2. \quad (6)$$

IV. COMPARISON OF THEORY WITH PREVIOUS EXPERIMENTS

Optical oscillator strengths and angular integrated cross sections are often used as a benchmark of theory and experiment. Therefore, we tested the theory first by calculating optical oscillator strengths (at 1500 eV incoming energy) and (angular) integrated cross sections at 400 and 500 eV. The results are compared with published experimental values in Tables I and II. The level of agreement varies, and significant discrepancies exist for the $5d$ excitations, indicating that these are very sensitive to the quality of the wave functions used.

As our main interest is in loss spectra at relatively high energies, we subsequently compare our calculations with the published work which is closest to the conditions of interest in this paper. Suzuki *et al.* [7,8,13] studied extensively

TABLE I. Optical oscillator strengths, as obtained experimentally by Suzuki *et al.* [7,8] and Chan *et al.* [9], compared to the values calculated with the present theory.

State	Expt. Suzuki <i>et al.</i>	Expt. Chan <i>et al.</i>	Calc.
$6s[3/2]_1^o$	0.222 ± 0.027	0.273 ± 0.014	0.313
$6s[1/2]_1^o$	0.158 ± 0.019	0.186 ± 0.009	0.161
$7s[3/2]_1^o$	0.0738 ± 0.011	0.0859 ± 0.0043	0.0646
$7s[1/2]_1^o$	–	–	0.0287
$5d[3/2]_1^o$	0.298 ± 0.045	0.379 ± 0.019	0.467
$5\bar{d}[3/2]_1^o$	–	–	0.508

TABLE II. Integrated cross section (in \AA^2) for different incoming energies E_0 , as obtained experimentally by Suzuki *et al.* [7,8], compared to the values calculated with the present theory.

State	E_0 (eV)	Expt. Suzuki <i>et al.</i>	Calc.
$6s[3/2]_1^o$	500	0.126 ± 0.015	0.179
$6s[3/2]_1^o$	400	0.148 ± 0.014	0.211
$6s[1/2]_1^o$	500	0.0751 ± 0.00019	0.0764
$6s[1/2]_1^o$	400	0.0899 ± 0.0011	0.0893
$7s[3/2]_1^o$	500	0.0323 ± 0.0048	0.0288
$7s[3/2]_1^o$	400	0.0378 ± 0.0057	0.0338
$5d[3/2]_1^o$	500	0.126 ± 0.019	0.204
$5d[3/2]_1^o$	400	0.148 ± 0.022	0.238

the scattering of 500 eV electrons from Xe at relatively small scattering angles ($\theta \leq 15^\circ$). In Fig. 2 we compare the results of our calculations with the spectrum of Suzuki for a scattering angle of 5.1° . The theory was broadened by the nominal resolution of the experiment [0.05 eV full-width-at-half-maximum (FWHM) Gaussian broadening]. Seventy-nine different final states were included. As noted previously, the intensity of those states which could only be populated by exchange scattering was negligibly small for the energies considered here. Suzuki *et al.* give the ratio of the intensity of the elastic peak and the inelastic peaks. We compare this ratio with the results for elastic and inelastic calculations, as described in the theory section. For the first observed level ($6s[3/2]_1^o$) the calculated intensity is 1.51% of the elastic peak, in very good agreement with the measured ratio (1.6%). The observed and calculated spectra agree quite well up to 11 eV in energy loss, with some peaks being about 30% lower in the theory compared to the experiment. Above 11 eV the agreement is somewhat less good. Here there is a myriad of different states, and not all were considered. However, some of the calculated intensities exceed the observed ones by a factor

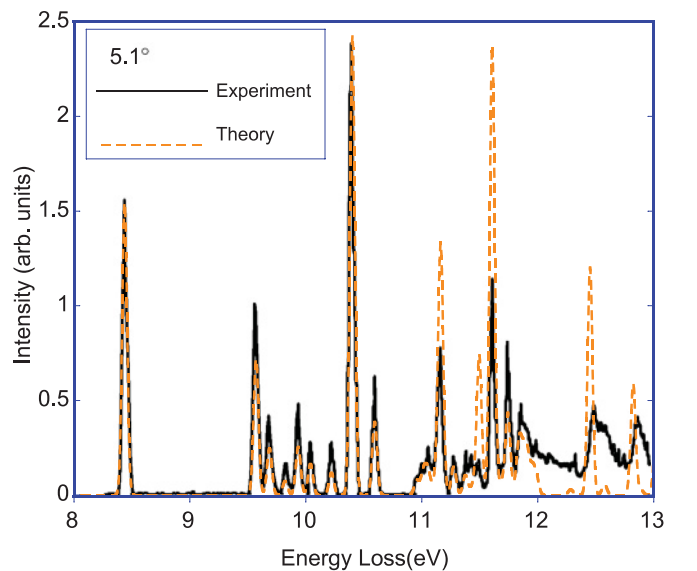


FIG. 2. (Color online) Comparison of the 500-eV spectra, taken for a scattering angle of 5.1° as measured by Suzuki *et al.* [13] with the RDW present theory.

of 2 or more. Above 12.1 eV the continuum starts, which was not considered in the theory. Coupling between this continuum and discrete states gives rise to the observed Fano profiles seen experimentally at the highest energy losses [14].

The angular dependence of the inelastic excitations, again plotted as a fraction of the elastic peak, are shown in Fig. 3 for both the present theoretical calculations and the experimental values of Suzuki *et al.* (where available). Agreement is very good for the $6s[3/2]_1^o$, $5d[3/2]_1^o$, and $5d[7/2]_3^o$ levels, whereas the theory seems to underestimate the $6s[1/2]_1^o$, $7s[3/2]_1^o$, and $5d[5/2]_3^o$ levels somewhat. Considering the large variation of the signal intensity (up to three orders of magnitude from

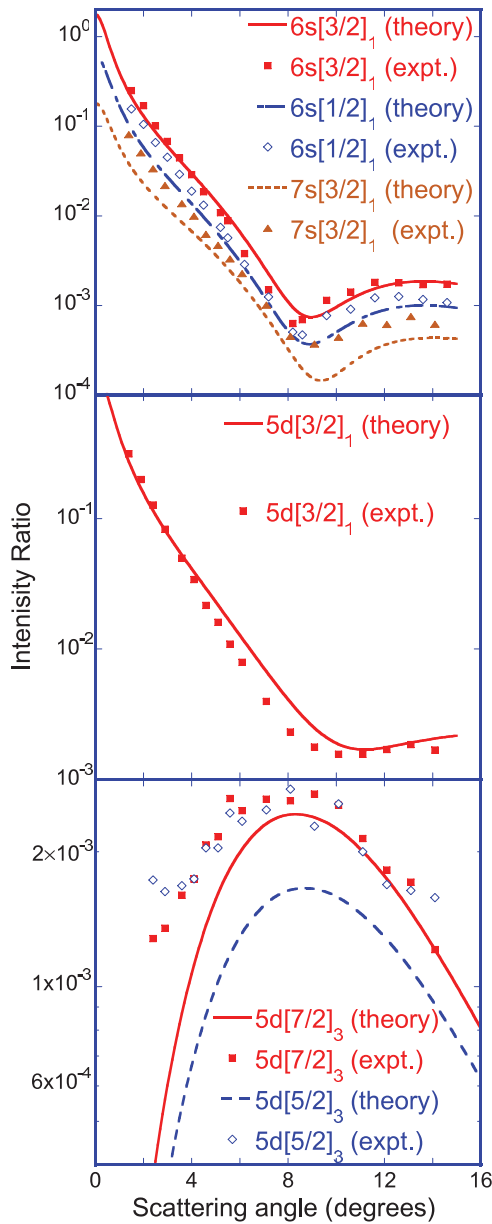


FIG. 3. (Color online) The intensity of the $6s$, $7s$, and $5d$ levels as a fraction of the elastic peak intensity for 500 eV electrons scattered from Xe. The experimental data are from Suzuki *et al.* [7,8], and the theoretical values are from the theory described here. Note that the $J = 1$ transitions are sharply forward peaked, in contrast to the $J = 3$ transitions.

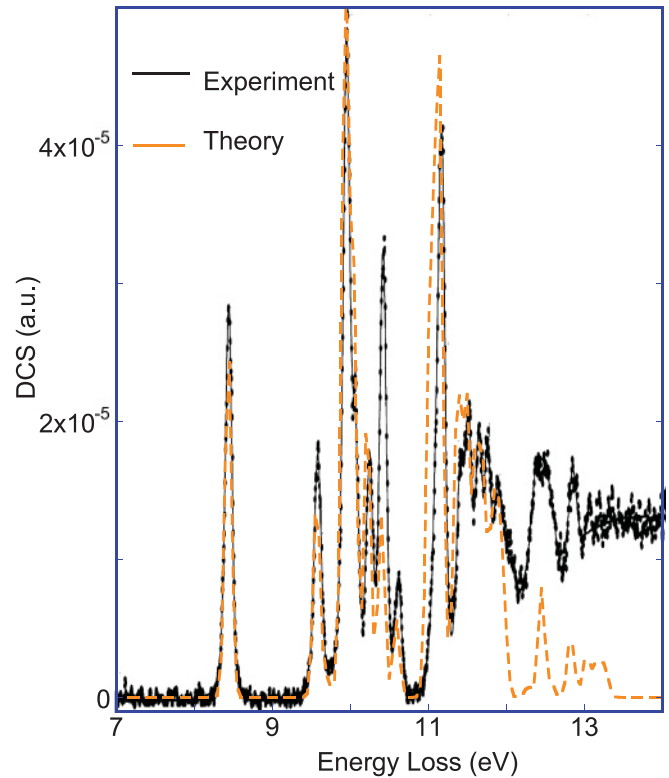


FIG. 4. (Color online) Comparison of the 500-eV spectra, taken for a scattering angle of 90° as measured by Urpelainen *et al.* with the present theory. Vertical scale of the experiment is arbitrary. The vertical scale of the theory is chosen in such a way that for nonoverlapping peaks the spectrum height corresponds to the differential cross sections in atomic units (a.u.).

0° to 15°) the obtained agreement is quite satisfactory. Note also the pronounced difference in behavior of the $J = 1$ dipole-allowed transitions and the $J = 3$ dipole-forbidden transitions. For an angle of $\theta = 8^\circ$, the former have decreased (from their maximum at $\theta = 0^\circ$) by three orders of magnitude, whereas the latter have a maximum at this angle and are effectively zero at $\theta = 0^\circ$.

Urpelainen *et al.* [15] measured 500 eV electrons scattered from Xe over larger angles (90°), with an energy resolution of 100 meV FWHM. Their results are compared with our calculations in Fig. 4. Here we have no information about the ratio of the elastic and inelastic signal strength, so the vertical scale of the experiment was adjusted to give the best agreement.

We also made a measurement with our spectrometer under these conditions (500 eV, 90°), which included the elastic peak as is shown in Fig. 5. Our resolution (350 meV FWHM) is good enough to resolve the $6s[3/2]_1^o$ state. We found the $6s[3/2]_1^o$ to the elastic peak ratio to be 1:872, about 30% less than the calculated ratio of 1:658.

To our knowledge, this is the first time that calculations have been used to construct a spectrum under these conditions, and, overall, we think the results are encouraging. Clearly, these distorted-wave calculations capture a lot of the physics of these large-angle scattering experiments with energetic electrons.

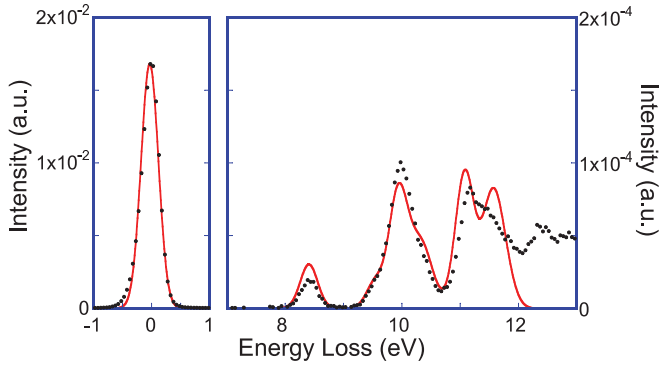


FIG. 5. (Color online) Comparison of the 500 eV spectra, taken for a scattering angle of 90° with a spectrum generated from the output of the ROP code (elastic peak) and RDW code (inelastic excitations). The experiment and theory are normalized on equal peak height for the elastic peak.

V. COMPARISON OF THEORY WITH THE CURRENT EXPERIMENT AT 750 EV

From here on, we focus on our measurements at 750 eV. We first compare the measured and calculated spectra for $\theta = 45^\circ$ and $\theta = 90^\circ$. Here we are away from any sharp resonances in the elastic differential cross section. The results are shown in Fig. 6. These measurements include the elastic peak and theory and experiment are normalized to have equal elastic peak area. Thus, the calculated overall intensity in the loss part of the spectrum agrees quite well, but the distribution of the intensity over the various components differs somewhat between theory and experiment.

So far, the theory presented here describes the measured spectra at 500 and 750 eV reasonably well. We now investigate if the theory describes the peculiar behavior of the inelastic intensity near the sharp minimum in the elastic cross section as reported in Ref. [2]. Comparison of experiment with theory is more straightforward if the measured spectra are at different angles but constant energy, rather than at different energies but a constant angle, as was the case in Ref. [2]. In order to make such measurements possible, we added the aforementioned new deflectors. We now demonstrate that the deflectors can be used to verify the existence of a sharp minimum in the elastic cross section near 135° and 750 eV.

For this purpose, we use a mixture of H_2 and Xe ($\approx 1\%$ Xe, 99% H_2). The contributions of H and Xe to the elastic peak are separated at 750 eV, 135° scattering due to the recoil effect. The recoil energy under these conditions (momentum transfer 13.7 a.u. or 25.9 \AA^{-1}) is 1.4 eV for scattering from H and 0.01 eV for scattering from Xe (m_{Xe}/m_H times smaller). This aspect was described extensively before [2,16]. The spectra are shown in Fig. 7. The zero of the energy scale was adjusted slightly so the first peak (corresponding to Xe) was at 0.01 eV. The second peak then appears at an energy loss of about 1.4 eV, as expected for electrons scattering effectively from a single H atom. For a deflector voltage of -2.5 eV the Xe/H peak ratio has a minimum, and the H peak is 7.3 times larger than the Xe peak. For a 20 eV deflector voltage the H peak is 7.0 times smaller than the Xe peak. The elastic H cross section is very close to the Rutherford cross section and changes very

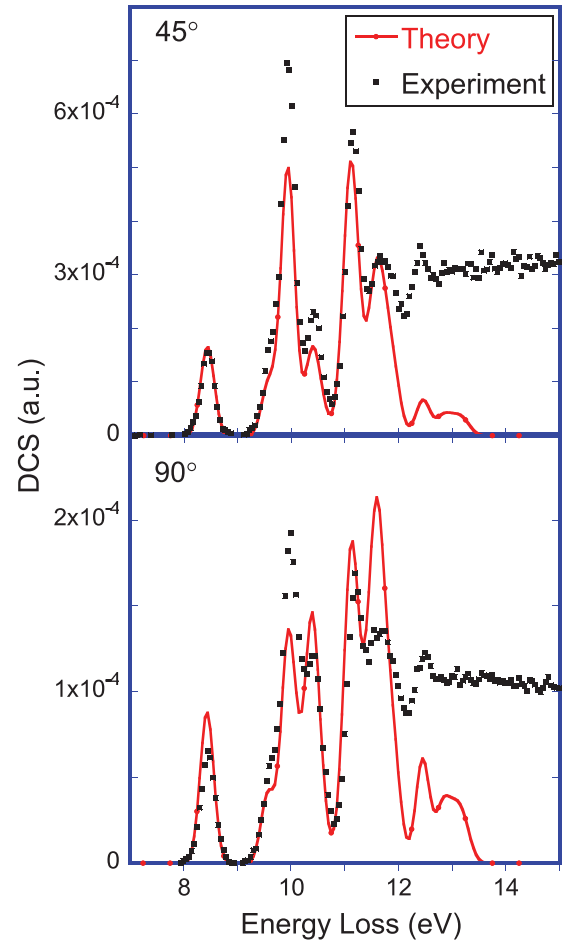


FIG. 6. (Color online) Comparison with theory of the 750 eV spectra, taken for scattering angles of 45° and 90° . The vertical scale is normalized to the elastic peak.

little over the angular range of interest (it decreases smoothly by 16% when θ increases from 130° to 140°). The observed changes in the Xe-H peak ratio are, thus, a clear sign of a sharp minimum in the Xe cross section near $\theta = 134.3 \pm 0.5^\circ$.

Neglecting the very small variation of the H cross section, we compare in Fig. 8 the observed intensity ratio with the calculated DCS using both the ELSEPA package [17] and the ROP method [10]. There is a small difference in the position of the minimum between the two calculations (132.2° for ELSEPA and 133.6° for ROP) and the experiment. This difference is about 2.2° between the experiment and the ELSEPA code and 0.7° between the experiment and the ROP method. The latter value is only slightly larger than the uncertainty in the scattering angle. Furthermore, at these large energies, the magnitude of the spin-flip scattering amplitude $g(\theta)$ [see Eq. (4)] is very small for all scattering angles θ and varies very slowly as a function of θ . On the other hand, the magnitude of the direct scattering amplitude $f(\theta)$ [see Eq. (3)] is a rapidly varying function of θ and exceeds that of the spin-flip amplitude everywhere except for a 1° interval surrounding this deep minimum in the DCS.

We next focus on the loss part of the spectrum of *pure* Xe near the minimum, and this is shown in the right panel of

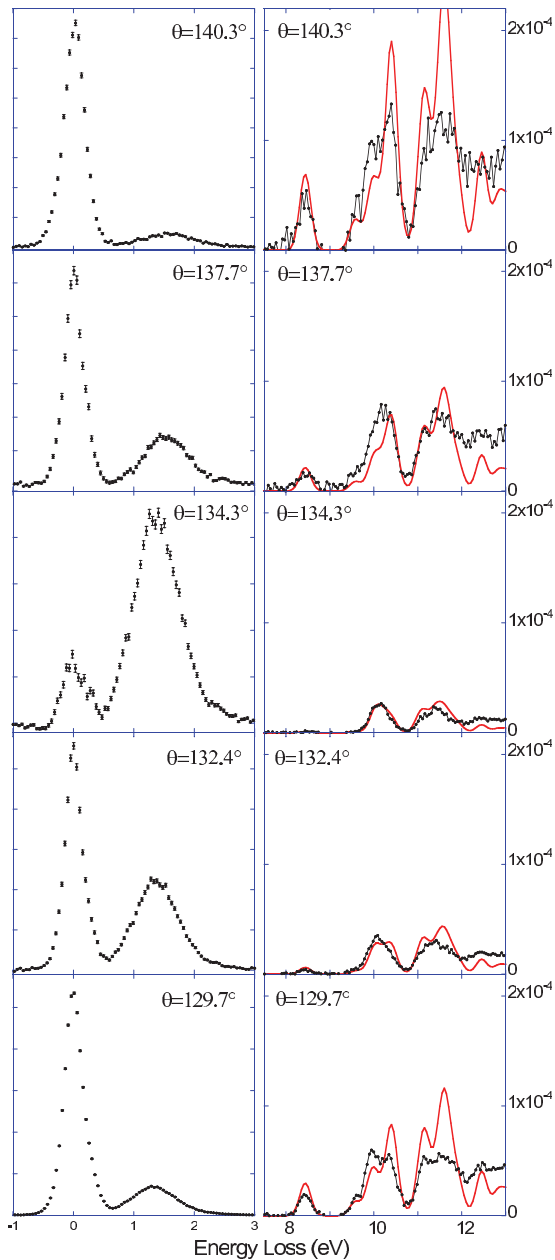


FIG. 7. (Color online) A comparison of the elastic peaks (in arbitrary units) of a Xe-H₂ gas mixture as a function of the scattering angle (left panels). The peak near 0 eV energy loss is associated with electrons scattered from Xe, the peak near 1.5 eV is due to electrons scattered from H. The right panels show the inelastic signal for pure Xe under these conditions and this is compared with calculations. Theory (in a.u.) and experiment are normalized using the calculated and measured elastic peak strength. See the main text for discussion of the offset in theoretical angle.

Fig. 7. Clearly, the shape of the loss part changes dramatically. For example, the $6s[3/2]_1^o$ state at 8.44 eV energy loss is quite pronounced away from the minimum but disappears in the noise at the minimum. In order to put the intensity here on an absolute scale, we use the simultaneously measured elastic peak intensity and the calculated elastic peak cross section. Clearly, there is an offset in the measured and observed

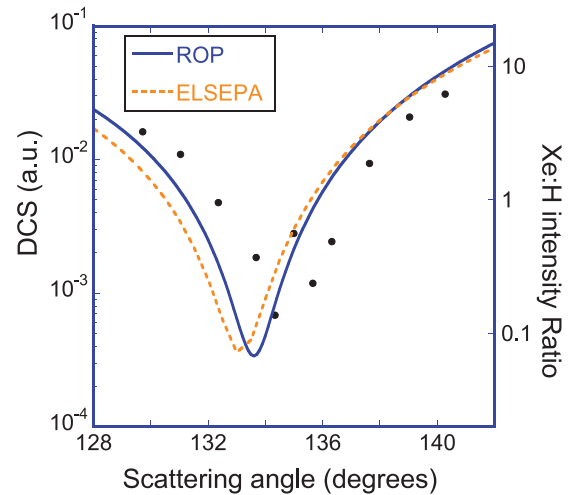


FIG. 8. (Color online) A comparison of the elastic differential cross section of 750-eV electrons as calculated using the ROP [10] and ELSEPA [17] programs (both with absorption) in the angular range corresponding to a pronounced dip in the elastic cross section. The experimentally obtained ratio of H and Xe elastic peak strength is shown as well (dots).

elastic DCS (see Fig. 8) and we have to account for this by a meaningful normalization.

Moreover, there is a strong correlation between the elastic DCS and the inelastic DCS of *certain* levels as can be seen in Fig. 9. Surprisingly, as the elastic and inelastic intensities are calculated using completely different theoretical approaches, the shape of the curves match very well for dipole-allowed ($J = 1$) transitions involving s states. In particular, the position of the minimum of the elastic-scattering cross section aligns very well with the minimum of the cross section of the dipole-allowed $J = 1$ excitations to s states and the $J = 0$ excitations to p states. The dip in the DCS is severely reduced for excitation to $J = 2$ p states and $J = 1$ d states. The dip is virtually absent for excitations to the $J = 3$ d states.

In light of the correlation of the elastic cross section with that of the inelastic excitations to the $J = 1$ s states, we decided to compare the measured spectrum at $\theta = 134.3^\circ$ (the experimental minimum of the elastic DCS) with the calculated spectrum at $\theta = 133.6^\circ$ (the calculated minimum of the elastic DCS and the minimum for $J = 1$ excitations to s states). For nearby results, we also apply a 0.7° offset between experiment and theory, as indicated in the right panel of Fig. 7. In this way theory and experiment are normalized to each other using the elastic DCS (using a 0.7° offset).

From the elastic peak intensity ratio of the Xe-H₂ mixture (and the knowledge that the H cross section does not vary sharply with angle under these conditions), we know that the Xe elastic DCS near 134.3° is reduced by a factor of ≈ 50 from its value near 140.3° or 129.7° . From the normalized loss spectra, we can see a similar reduction for the $6s[3/2]_1^o$ intensity near 8.4 eV. The DCS near 10 eV (due to several overlapping states) is reduced by only a factor of approximately 5.

The results of the calculations, normalized using the calculated elastic cross sections (using the ROP method) are

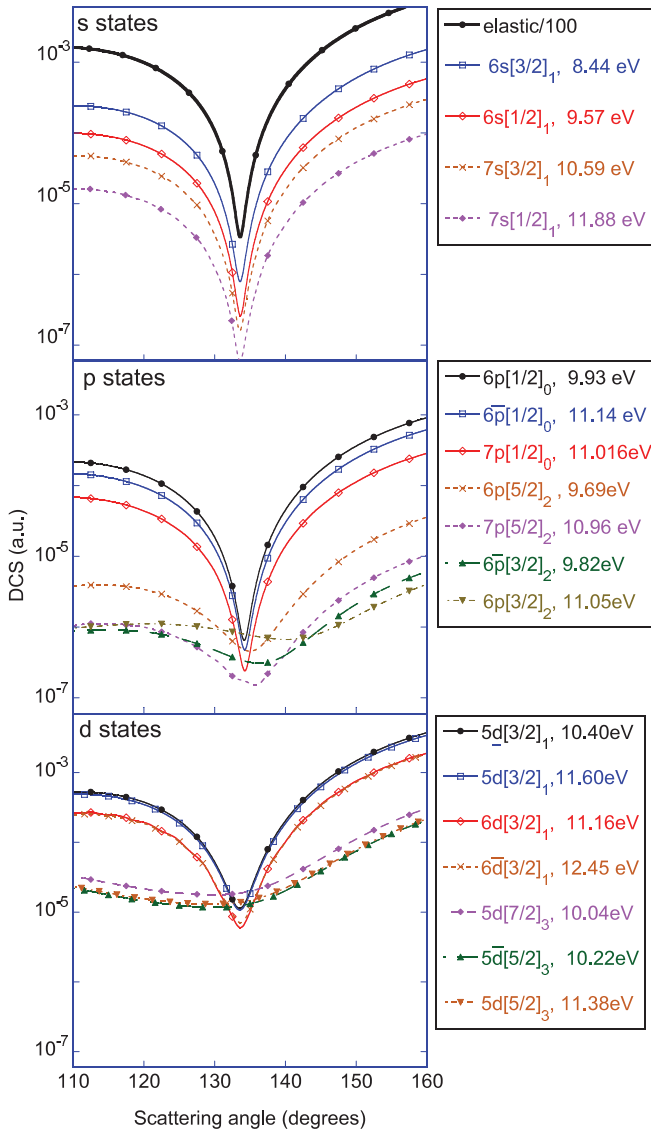


FIG. 9. (Color online) The calculated DCS for elastic scattering and several inelastic channels for 750-eV electrons in the angular region of the pronounced dip in the elastic DCS.

plotted in Fig. 7. The general trend in intensity versus angle is well reproduced, but details of the distribution of the intensity over the various states clearly differ between experiment and theory. The agreement between theory and experiment for the first feature ($6s[3/2]_1^o$ state at 8.4 eV) is very good, but, again, the level of agreement seems to decrease with increasing energy loss. Here measurements with improved resolution would be very helpful to determine the systematics of the discrepancy between theory and experiment.

VI. DISCUSSION AND CONCLUSIONS

Inelastic scattering of electrons with an energy of several hundred eV from noble gases has attracted little theoretical attention, despite the existence of sizable body of published experimental work (see Ref. [18] for a brief recent review of this topic). Deviations from the first Born approximation become evident when the momentum transfer exceeds 1 a.u.. In Ref. [4] we showed for Ne and Ar that calculations based on the distorted-wave framework give a reasonable description of the outermost excitations. Here we use the same theory for scattering from Xe but extend our comparison to deeper excitation energies below the continuum. This approach is reasonably successful under conditions where the first Born approximation is quite good (5.1°, 500 eV [13]), and under conditions where the first Born approximation fails completely (90°, 500 eV [15]).

Xe displays deep minima in the elastic differential cross section for certain angles and energies. The distorted-wave calculations show that the cross sections of certain final states (in particular $J = 1$ s states, and $J = 0$ p states) have similar minima as the elastic DCS. Less pronounced minima are found for $J = 2$ p states and $J = 1$ d states, whereas cross sections for the $J = 3$ d states are relatively smooth. These findings line up reasonably well with the qualitative two-step model of Ref. [2]. This two-step model (elastic deflection and inelastic excitation) predicts that those inelastic excitations with a strongly peaked cross section at $\theta = 0$ will have, at large angles, a DCS with minima as pronounced as those in the elastic channel.

The calculations presented here show that the s , p , or d nature of the excited state is important as well. For example, the $5d[3/2]_1^o$ transition is sharply peaked at 0° (see Fig. 3 for a comparison to experiment at 500 eV) but near 135°, 750 eV the DCS shows a broader, less-deep minimum compared to that of the elastic DCS, whereas the $6p[1/2]_0$ state does not have a strong peak in the DCS at 0°, but the DCS at 135° and 750 eV reflects the minimum in the elastic DCS quite well. The correlation seems to be stronger with the extent of the excited state wave function in momentum space rather than the DCS near 0°.

In conclusion, the distorted-wave approach describes the experimental results quite well. In particular, the peculiar changes in shape and intensity of the loss spectra near the sharp minimum of the elastic DCS are reproduced, indicating that elastic and inelastic processes are not as independent as is often (implicitly) assumed.

ACKNOWLEDGMENTS

The authors thank Mr. Avnish Anand for assistance with the measurements of the Xe-H₂ mixture and Professor Weigold for critically reading the manuscript. The research was made possible by funding from the Australian Research Council.

[1] F. Salvat, *Phys. Rev. A* **68**, 012708 (2003).

[2] M. Vos, *J. Phys. B* **43**, 215201 (2010).

[3] W. Werner, K. Glantschnig, and C. Ambrosch-Draxl, *J. Phys. Chem. Ref. Data* **38**, 1013 (2009).

[4] M. Vos, R. P. McEachran, G. Cooper, and A. P. Hitchcock, *Phys. Rev. A* **83**, 022707 (2011).

[5] *Simion Version 8*, Scientific Instrument Services, Inc. (2008).

- [6] I. P. Grant, B. J. McKenzie, P. H. Norrington, D. F. Mayers, and N. C. Pyper, *Comput. Phys. Commun.* **21**, 207 (1980).
- [7] T. Y. Suzuki, Y. Sakai, B. S. Min, T. Takayanagi, K. Wakiya, H. Suzuki, T. Inaba, and H. Takuma, *Phys. Rev. A* **43**, 5867 (1991).
- [8] T. Y. Suzuki, H. Suzuki, F. J. Currell, S. Ohtani, T. Takayanagi, and K. Wakiya, *Phys. Rev. A* **53**, 4138 (1996).
- [9] W. F. Chan, G. Cooper, X. Guo, G. R. Burton, and C. E. Brion, *Phys. Rev. A* **46**, 149 (1992).
- [10] S. Chen, R. P. McEachran, and A. D. Stauffer, *J. Phys. B* **41**, 025201 (2008).
- [11] R. P. McEachran and A. D. Stauffer, *J. Phys. B* **23**, 4605 (1990).
- [12] R. P. McEachran and A. D. Stauffer, *Aust. J. Phys.* **50**, 511 (1997).
- [13] T. Y. Suzuki, H. Suzuki, S. Ohtani, T. Takayanagi, and K. Okada, *Phys. Rev. A* **75**, 032705 (2007).
- [14] U. Fano and J. W. Cooper, *Rev. Mod. Phys.* **40**, 441 (1968).
- [15] S. Urpelainen, M. Huttula, P. Kovala, A. Makinen, A. Calo, S. Aksela, and H. Aksela, *J. Electron Spectrosc. Relat. Phenom.* **156–158**, 145 (2007).
- [16] M. Vos and M. Went, *J. Phys. B* **42**, 065204 (2009).
- [17] F. Salvat, A. Jablonski, and C. J. Powell, *Comput. Phys. Commun.* **165**, 157 (2005).
- [18] L.-F. Zhu, *J. Phys: Conf. Ser.* **235**, 012007 (2010).